Demonstration of Marginal Stability Theory by a 200–kW Second-Harmonic Gyro-TWT Amplifier

Q. S. Wang,* D. B. McDermott, and N. C. Luhmann, Jr.
Department of Applied Science, University of California, Davis, California 95616
(Received 7 August 1995)

A recent theory for achieving stability in high-power gyrotron traveling wave (gyro-TWT) amplifiers has been verified. By keeping the interaction length shorter than the critical oscillation length for the competing modes, stability was achieved. The experiment also verified the theoretical prediction that harmonic gyro-TWT's can produce higher power because their weaker interaction yields a higher threshold electron current for oscillation. The second-harmonic gyro-TWT single-stage amplifier stably generated 207 kW, nearly twice the level achieved by fundamental-harmonic gyro-TWT's at a comparable voltage.

PACS numbers: 85.10.Jz, 42.52.+x

The gyrotron traveling wave (gyro-TWT) amplifier [1] has attracted considerable attention because of its potential to efficiently generate high power in the millimeter wavelength region due to the power handling capability of its oversized, unloaded fast-wave interaction waveguide. In a gyro-TWT amplifier, electrons gyrate along a properly tuned, axial magnetic field and synchronously interact with and amplify a copropagating electromagnetic wave whose frequency satisfies $\omega = s\Omega_{co} + k_{\|}v_{\|}$, where Ω_c is the electron cyclotron frequency, s is the harmonic number, and $k_{\|}v_{\|}$ represents the Doppler shift. The wave is amplified in this negative-mass instability because the electrons bunch due to the inverse dependence of the cyclotron frequency on the relativistic Lorentz factor. Experimental devices operating at the fundamental frequency ($\omega = \Omega_c$) and in the fundamental mode of the interaction waveguide have produced 120 kW at 5 GHz [2] and 62 kW at 35 GHz [3]. Unfortunately, the tremendous potential of this high gain, broadband amplifier has to date been only partially realized because of its propensity to oscillate in the operating mode [4,5], as well as in other modes at other cyclotron harmonics [6].

A marginal stability theory [7] was recently introduced to maximize the power level and gain of stable gyro-TWT amplifiers. First, the electron beam current is reduced below the threshold value at which the operating mode is excited at the cutoff frequency due to the forward-wave bandwidth extending into the backward-wave region. The interaction length of the amplifier is then chosen to be shorter than the critical oscillation length for the strongest competing interaction. The marginal stability theory also predicts that harmonic gyro-TWT's are capable of significantly higher power than at the fundamental, because the stronger fundamental-harmonic interaction restricts the beam current to low levels for stability. Harmonic gyrotron devices are also valuable because they significantly reduce the strength of the required magnetic field. An eighth-harmonic gyro-TWT amplifier experiment [8] reduced the requisite magnetic field by a factor of 8. However, it was not designed for high power or stability. The purpose of the experiment reported herein was to verify the marginal stability theory and to realize a high power, stable, second-harmonic gyro-TWT amplifier.

The second-harmonic device was designed [9] to amplify the TE_{21} mode of circular waveguide, because then no oscillation can occur at the first harmonic [8], as can be seen in the amplifier's dispersion diagram shown in Fig. 1. If the magnetic field is set to the grazing value B_g, where the second-harmonic cyclotron resonance line grazes the TE_{21} mode, as is desired for broadband operation, then the fundamental harmonic resonance line is well below the lowest order mode (TE_{11}). For the desired $TE_{21}^{(2)}$ interaction (the superscript refers to the harmonic number), there will be a finite width of unstable spectrum about the intersection. If this unstable band is confined to the forward-wave region ($k_{\|} > 0$), waves in the TE_{21} mode will convectively grow in amplitude down the interaction region. However, if the interaction

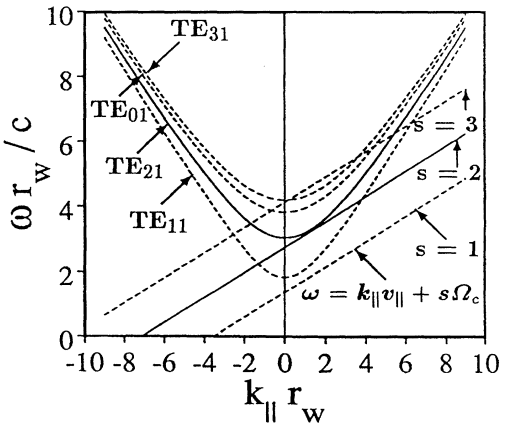

FIG. 1. Uncoupled dispersion relation of the operating mode (intersection of unbroken curves) and possible oscillating modes (intersections of broken curves with negative $k_{\|}$) for $TE_{21}^{(2)}$ gyro-TWT amplifier.

 0031-9007/95/75(23)/4322(4)$06.00

strength is sufficiently strong that the unstable band extends into the backward-wave region ($k_{\|} < 0$), waves in the backward direction will grow from noise due to internal feedback to yield oscillation near the cutoff frequency [10]. In this absolute instability [5], the wave grows in time at all spatial positions. The threshold value of electron beam current for the onset of oscillation is shown in Fig. 2 for the three lowest harmonic $TE_{n1}^{(n)}$ interactions for a beam guiding center-to-wall-radius ratio of $r_c/r_w = 0.4$. The threshold current monotonically increases with decreasing transverse to axial velocity ratio $v_\perp/v_{\|}$ and shows a very strong functional dependence on it. Mathematically a lower $v_\perp/v_{\|}$ value results in a steeper slope for the cyclotron resonance line, so that the grazing intersection point is shifted away from the cutoff where the absolute instability is strongest, while physically, a smaller $v_\perp/v_{\|}$ ratio corresponds to a beam with less free transverse energy to give up and, therefore, the system will be weaker in gain, less efficient, and more stable to the absolute instability. A high voltage (1 MV) first-harmonic gyro-TWT with $v_\perp/v_{\|} \approx 0.4$ that operated in this regime was able to generate an output power of 20 MW [11].

As the electron beam current must be maintained below the threshold value to ensure stability, the output power capability of a moderate voltage ($\leq$100 kV), fundamental-harmonic gyro-TWT is greatly limited. However, a harmonic gyro-TWT has a weaker interaction strength and can therefore be operated with a much higher value of current as shown in Fig. 2. Specifically, a harmonic gyro-TWT amplifier is more stable to self-oscillation due to the absolute instability than a fundamental-harmonic gyro-TWT. As a result, a harmonic gyro-TWT can stably generate significantly higher output power than a fundamental-frequency gyro-TWT for a given beam voltage and velocity ratio.

In addition to absolute oscillation, a gyro-TWT amplifier is also susceptible to self-oscillation as a gyrotron backward-wave oscillator (gyro-BWO) [12], which can be excited at intersections of the waveguide dispersion and harmonic cyclotron resonance lines [6] in the negative-$k_{\|}$ region. For a sufficiently long interaction circuit, a resonant wave propagating counter to the streaming direction of the electrons will grow from noise. In a second-harmonic gyro-TWT amplifier with the dispersion relations shown in Fig. 1, harmonic gyro-BWO oscillations can occur in various modes, including the $TE_{11}^{(2)}$, $TE_{31}^{(3)}$, $TE_{41}^{(4)}$, etc. The critical lengths [13] for oscillation of the strongest modes are shown in Fig. 3. By limiting the interaction circuit to a length less than the shortest critical length, a gyro-TWT amplifier can be kept stable. If the limiting critical length is too short to allow amplification with the desired gain, several of these stable sections separated by attenuators [14] for isolation can be employed. Alternatively, if the odd-order azimuthal modes can be stabilized, high gain amplification will be possible in a single-stage interaction circuit whose length is now limited by the critical length for the much weaker, $TE_{41}^{(4)}$ oscillation mode.

To suppress the odd-order azimuthal modes, the circular interaction waveguide was sliced axially with two cuts separated in azimuth by 90°. A dielectric cylinder coated with graphite was inserted in the annulus between the interaction circuit and vacuum envelope to absorb the waves leaking through the slices. The insertion loss through the 65-cm length interaction circuit for the TE_{11} mode at the most likely oscillation frequency was measured to exceed 24 dB, while the insertion loss of the operating TE_{21} mode through the entire system, excluding the input and output couplers, is below 1.5 dB over the frequency band of interest. Although the loss of the TE_{31} mode was not measured, a high attenuation similar to that of the TE_{11} mode is expected because of their similar symmetry.

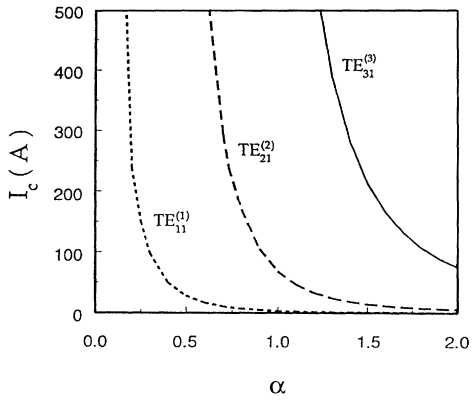

FIG. 2. Dependence of start-oscillation current on velocity ratio $\alpha = v_\perp/v_{\|}$ for absolute instability in fundamental, second- and third-harmonic $TE_{n1}^{(n)}$ gyro-TWT amplifiers (80 kV, $B/B_g = 0.97$).

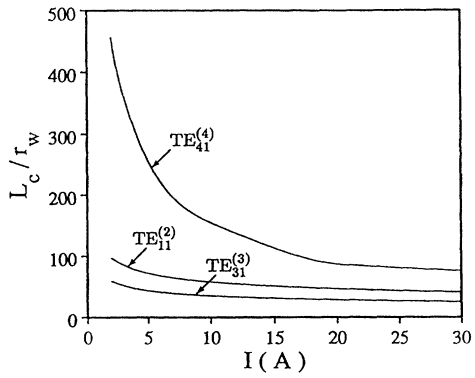

FIG. 3. Dependence of critical length on beam current for backward-wave oscillations at second harmonic in TE_{11} mode, third harmonic in TE_{31} mode, and fourth harmonic in TE_{41} mode (100 kV, $v_\perp/v_{\|} = 1$, $B/B_g = 0.98$, $r_c/r_w = 0.4$).

A schematic of the second-harmonic gyro-TWT experimental apparatus [15] is shown in Fig. 4. An 80-kV, annular electron beam is emitted from a single anode, magnetron injection gun (MIG) during a 2-μs pulse and propagates through a magnetic compression region where the electrons' axial velocity is partially converted into transverse velocity with a final $v_\perp/v_\parallel \approx 1$. To avoid fundamental gyrotron oscillation in the system, the lowest order cutoff frequency of each individual section is larger than the corresponding fundamental electron cyclotron frequency. The electrons enter the circuit with $r_c/r_w = 0.4$ and interact continuously with a linearly polarized TE_{21} wave launched by a nominal 1-dB directional coupler, which was measured to have a selectivity of 99% to the TE_{21} mode. Resonance is well maintained in the interaction region since the magnetic field's uniformity here is $\pm 0.5\%$. Half of the amplified RF power is extracted for diagnosis through a similar 3-dB directional coupler at the output end and the other half is absorbed by an RF load.

Directional couplers are attached to both the input and output windows to enable measurement of either the forward or backward waves. The power measurements are made with well-calibrated crystal detectors, directional couplers, and precision variable attenuators. A heterodyne receiver determines the frequency content of the output. The RF drive is provided by a 1-kW, 12–18-GHz helix TWT amplifier. The spent electron beam is gathered by a beam collector connected to ground through a noninductive resistor. The collected current can be compared with the emitted current measured by a Rogowski loop. The voltage applied to the electron gun is measured by a capacitive probe.

The amplifier was operated with an electron beam current up to 20 A, which is below the theoretically predicted threshold current for the absolute instability of 28 A. By varying the axial magnetic field, the amplifier can be tuned for optimum gain or optimum efficiency. In the first case, the magnetic field is set to the grazing value, where the electrons travel at the same velocity as the group velocity of the wave, which yields the strongest interaction. A peak small-signal gain of 38 dB was measured. When the magnetic field is reduced from the grazing value, a higher efficiency and output power is obtained.

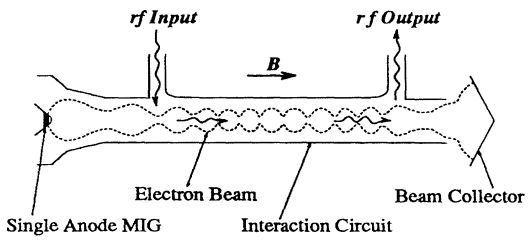

FIG. 4. Schematic of the second-harmonic gyro-TWT amplifier experimental system.

The transfer curve of the $TE_{21}^{(2)}$ gyro-TWT amplifier at 15.7 GHz is shown in Fig. 5 with the magnetic field set for optimum efficiency. The amplifiers output power grows linearly with increasing input power in the small-signal regime, resulting in a linear gain of 22 dB for a 20-A beam. For higher RF drive power, the amplifier eventually saturates as the trapped electrons move into the accelerating phase of the RF field and begin to recover their energy from the wave. As expected, an electron beam of lower current yields a lower linear growth rate and saturates for a higher level of RF input power. For the case of a 20-A beam, a saturated gain of 16 dB was obtained.

The saturated bandwidth of the amplifier was obtained by adjusting the RF input power at each frequency to maximize the output power and is shown in Fig. 6. The magnetic field was adjusted for the highest efficiency at 15.7 GHz and then held fixed for measurements at other frequencies. The measured 3-dB bandwidth is 2.1%. Figure 6 shows that an output power level of 207 kW is generated by the second-harmonic TE_{21} gyro-TWT amplifier, which is significantly higher than the highest power reported for a stable, moderate voltage, fundamental-harmonic gyro-TWT amplifier [2]. The 207-kW output power corresponds to a device efficiency of 12.9%.

The high power amplifier is found to be completely stable for zero RFD drive power. No oscillation can be detected within the measurement sensitivity of 20 mW for the operating parameters of Figs. 5 and 6. However, oscillation in the operating mode due to the absolute instability can be induced by increasing the axial magnetic field. Oscillation in other modes was never observed. The gyro-TWT amplifier with a mode-selective

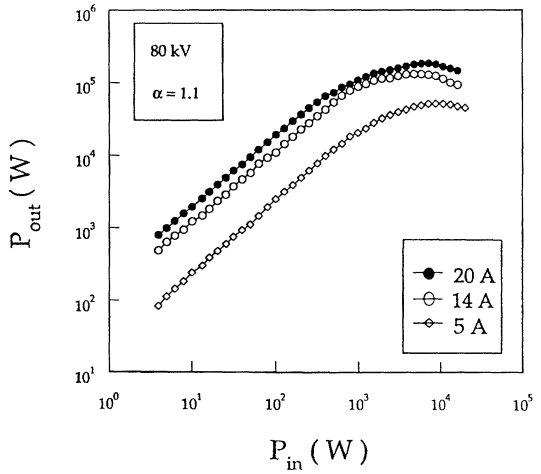

FIG. 5. Measured transfer curve of second-harmonic TE_{21} gyro-TWT amplifier at a magnetic field of 2.9 kG and a frequency of 15.7 GHz for several values of electron beam current (I = 5, 14, and 20 A for 80 kV and $v_\perp/v_\parallel = 1.1$).

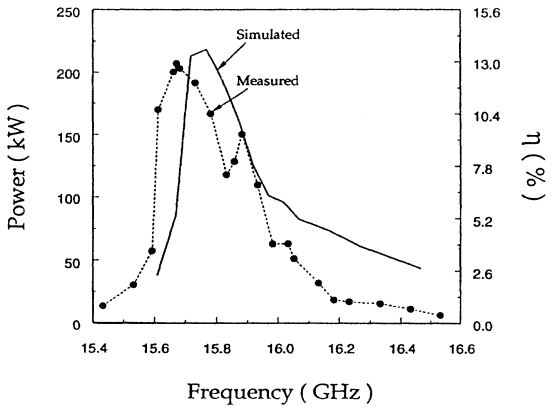

FIG. 6. Measured saturated bandwidth of the second-harmonic TE_{21} gyro-TWT amplifier (solid points) compared with simulation results (solid curve) for an 80-kV, 20-A beam with $v_\perp/v_\parallel = 1.1$ and $\Delta v_\parallel/v_\parallel = 14\%$ in a magnetic field of $B/B_g = 0.97$.

and length-limited interaction circuit had effectively been made stable from potential gyro-BWO oscillations.

A nonlinear self-consistent code [9] was used to simulate the amplifier's performance to determine the beam's axial velocity spread. The simulation results for an 80-kV, 20-A, $v_\perp/v_\parallel = 1.1$ beam with $r_c/r_w = 0.4$ and an axial velocity spread of 14% in a magnetic field of $B_0 = 0.97B_g$ have also been included in Fig. 6. The theory agrees quite well with the experimental results. The small discrepancy between the two bandwidths may be due to a shift of the cutoff frequency from fabrication errors or that the actual beam has a slightly higher value of $v_\perp/v_\parallel$. For these values, the predicted small-signal gain of 21.1 dB at 15.7 GHz is also in good agreement with the experimental value of 22 dB, especially when the regenerative gain from the finite circuit mismatches is considered. Since the amplifier had been predicted to generate 400 kW with a bandwidth of 5% for an axial velocity spread of 8%, it is evident that the relatively high velocity spread has limited the output power level as well as the bandwidth.

Motivated by the recent marginal stability theory that a harmonic gyro-TWT is more stable to spontaneous oscillation than a fundamental-harmonic gyro-TWT and therefore has increased capability for high power generation, a second-harmonic gyro-TWT amplifier experiment was conducted that generated an output power in excess of 200 kW in Ku band with a peak efficiency of 12.9%. The measured saturated gain and bandwidth are 16 dB and 2.1%, respectively. The success of the experiment has not only confirmed the validity and usefulness of the theory as a procedure for achieving stability in a high performance gyro-TWT but also demonstrated a second-harmonic gyro-TWT amplifier with a stable RF output power nearly twice that of the highest power, stable fundamental-frequency gyro-TWT at a comparable voltage. As coherent high power microwave and millimeter-wave sources, harmonic gyro-TWT amplifiers are viable and promising. The concept that harmonic gyro-TWT's are capable of higher power can be further extended. To take advantage of the higher stable beam currents that are predicted in Fig. 2 for third-harmonic interaction, a higher power, third-harmonic TE_{31} gyro-TWT amplifier has recently been designed [16] that is predicted to stably generate 1 MW at 140 GHz with an efficiency of 19% and a bandwidth of 6%.

This work has been supported by AFOSR under Grant No. F49620-94-1-0396 and by ARO under contract No. DAAH04-93-G-0084. The authors would like to express their gratitude to Professor K. R. Chu and Professor C. S. Kou and Dr. L. R. Barnett for their generous support in the construction of the electron gun and their insightful suggestions.

*Present address: Micramics, Inc., Cupertino, CA 95014.

[1] K. R. Chu, A. T. Drobot, H. H. Szu, and P. Sprangle, IEEE Trans. Microwave Theory Tech. **28**, 313 (1980).

[2] R. S. Symons, H. R. Jory, J. Hegji, and P. E. Ferguson, IEEE Trans. Microwave Theory Tech. **29**, 181 (1981).

[3] K. R. Chu, L. R. Barnett, H. Y. Chen, S. H. Chen, Ch. Wang, Y. S. Yeh, Y. C. Tsai, T. T. Yang, and T. Y. Dawn, Phys. Rev. Lett. **74**, 1103 (1995).

[4] L. R. Barnett, J. M. Baird, Y. Y. Lau, K. R. Chu, and V. L. Granatstein, Tech. Dig. Int. Electron Devices Meet. **1616-2**, 314 (1980).

[5] Y. Y. Lau, K. R. Chu, L. R. Barnett, and V. L. Granatstein, Int. J. Infrared Millimeter Waves **2**, 373 (1981).

[6] L. R. Barnett, L. H. Chang, H. Y. Chen, K. R. Chu, W. K. Lau, and C. C. Tu, Phys. Rev. Lett. **63**, 1062 (1989).

[7] A. T. Lin, K. R. Chu, C. C. Lin, C. S. Kou, D. B. McDermott, and N. C. Luhmann, Jr., Int. J. Electron. **72**, 873 (1992).

[8] D. S. Furuno, D. B. McDermott, C. S. Kou, N. C. Luhmann, Jr., and P. Vitello, Phys. Rev. Lett. **62**, 1314 (1989).

[9] Q. S. Wang, C. S. Kou, D. B. McDermott, A. T. Lin, K. R. Chu, and N. C. Luhmann, Jr., IEEE Trans. Plasma Sci. **20**, 163 (1992).

[10] R. J. Briggs, *Electron Stream Interaction with Plasma* (MIT Press, Cambridge, 1964), Chap. 2.

[11] S. H. Gold, D. A. Kirkpatrick, A. W. Fliflet, R. B. McCowan, A. K. Kinkead, D. L. Hardesty, and M. Sucy, J. Appl. Phys. **69**, 6696 (1991).

[12] S. Y. Park, V. L. Granatstein, and R. K. Parker, Int. J. Electron. **57**, 1109 (1984).

[13] C. S. Kou, Q. S. Wang, D. B. McDermott, A. T. Lin, K. R. Chu, and N. C. Luhmann, Jr., IEEE Trans. Plasma Sci. **20**, 155 (1992).

[14] A. K. Ganguly and S. Y. Ahn, IEEE Trans. Electron Devices **31**, 474 (1984).

[15] Q. S. Wang, Ph.D. thesis, University of California, Los Angeles, 1995.

[16] Q. S. Wang, D. B. McDermott, C. K. Chong, C. S. Kou, K. R. Chu, and N. C. Luhmann, Jr., IEEE Trans. Plasma Sci. **22**, 608 (1994).